Electronic Supplementary Information (ESI)

Two unique copper cluster-based metal-organic frameworks with high performance for CO_2 adsorption and separation

Jiaqi Yuan,[a] Jiantang Li,[a] Songtian Che,[b] Guanghua Li,[a] Xinyao Liu,[a] Xiaodong Sun,[a] Lifei Zou,[a] Lirong Zhang[a, *] and Yunling Liu[a, *]

[a] *State Key Laboratory of Inorganic Synthesis and Preparative Chemistry, College of Chemistry, Jilin University, Changchun 130012, P. R. China. Fax: +86-431-85168624; Tel: +86-431-85168614; E-mail: yunling@jlu.edu.cn, zlr@jlu.edu.cn.*

[b] *Department of Ocular Fundus Disease of the Second Clinical Hospital, Jilin University, Changchun 130022, P. R. China.*

S1. Calculation procedures of selectivity from IAST

The measured experimental data is excess loadings (q^{ex}) of the pure components CO_2, CH_4, C_2H_6 and C_3H_8 for compound **1**, which should be converted to absolute loadings (q) firstly.

$$q = q^{ex} + \frac{pV_{pore}}{ZRT}$$

Here Z is the compressibility factor. The Peng-Robinson equation was used to estimate the value of compressibility factor to obtain the absolute loading, while the measure pore volume 0.40 $cm^3\ g^{-1}$ is also necessary.

The dual-site Langmuir-Freundlich equation is used for fitting the isotherm data at 298 K.

$$q = q_{m_1} \times \frac{b_1 \times p^{1/n_1}}{1 + b_1 \times p^{1/n_1}} + q_{m_2} \times \frac{b_2 \times p^{1/n_2}}{1 + b_2 \times p^{1/n_2}}$$

Here p is the pressure of the bulk gas at equilibrium with the adsorbed phase (kPa), q is the adsorbed amount per mass of adsorbent (mol kg^{-1}), q_{m1} and q_{m2} are the saturation capacities of sites 1 and 2 (mol kg^{-1}), b_1 and b_2 are the affinity coefficients of sites 1 and 2 (1/kPa), n_1 and n_2 are the deviations from an ideal homogeneous surface.

The selectivity of preferential adsorption of component 1 over component 2 in a mixture containing 1 and 2, perhaps in the presence of other components too, can be formally defined as

$$S = \frac{q_1/q_2}{p_1/p_2}$$

q_1 and q_2 are the absolute component loadings of the adsorbed phase in the mixture. These component loadings are also termed the uptake capacities. We calculate the values of q_1 and q_2 using the Ideal Adsorbed Solution Theory (IAST) of Myers and Prausnitz.

S2. Supporting Figures

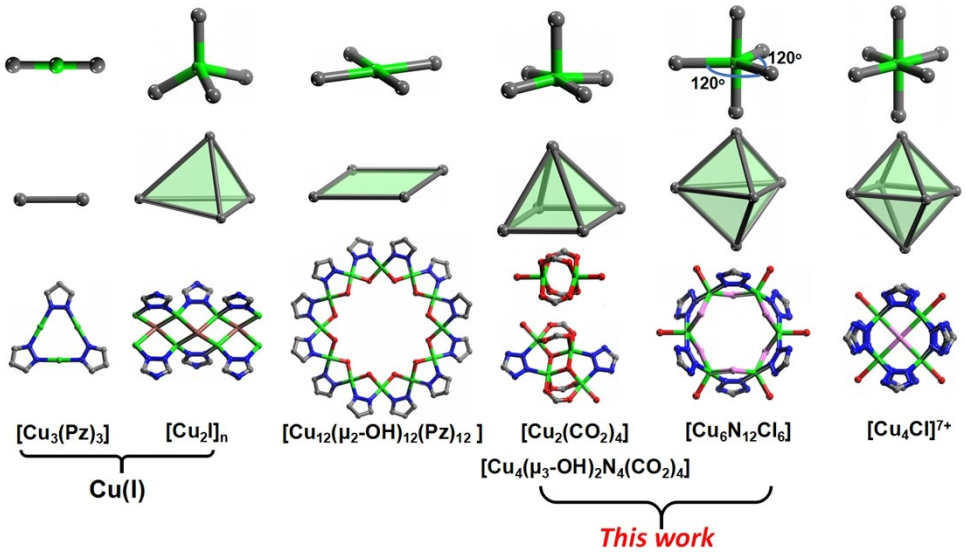

Fig. S1 Comparison of Cu atom coordination modes for reported Cu-MOFs and this work.

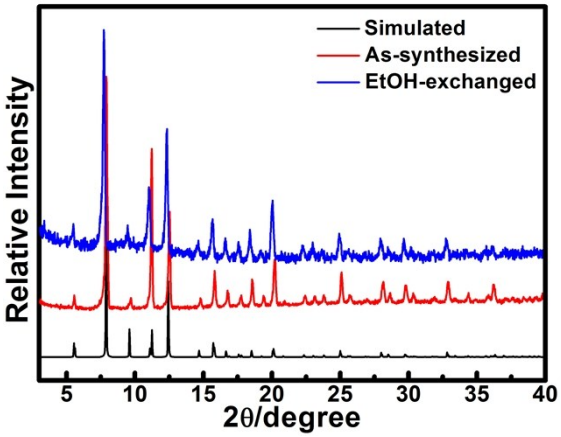

Fig. S2 PXRD patterns of compound **1** for simulated, as-synthesized and EtOH-exchanged samples. The differences in reflection intensity are probably due to preferred orientations in the powder sample.

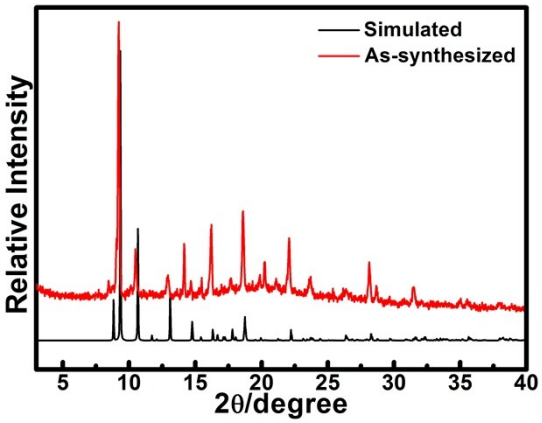

Fig. S3 PXRD patterns of compound **2** for simulated and as-synthesized samples. The differences in reflection intensity are probably due to preferred orientations in the powder sample.

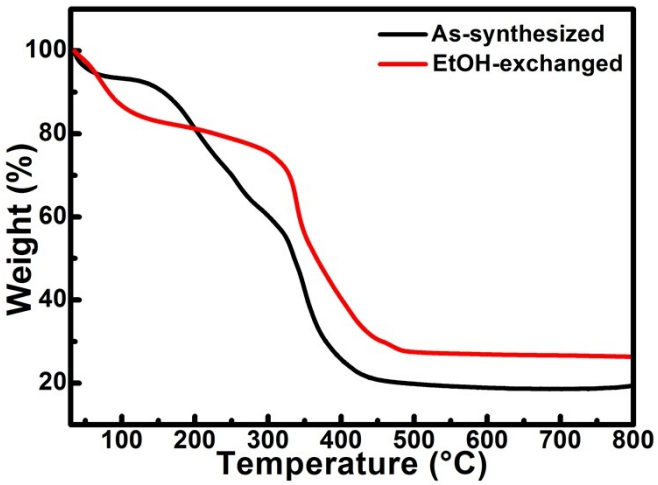

Fig. S4 Thermogravimetric analysis curves of compound **1** for the as-synthesized and EtOH-exchanged samples.

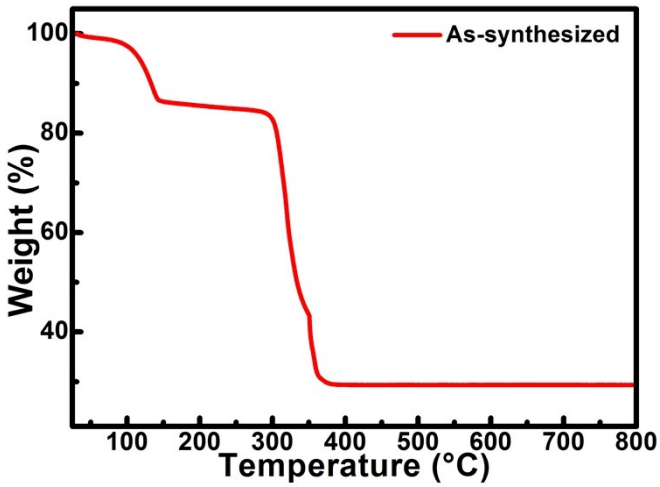

Fig. S5 Thermogravimetric analysis curve of compound **2**.

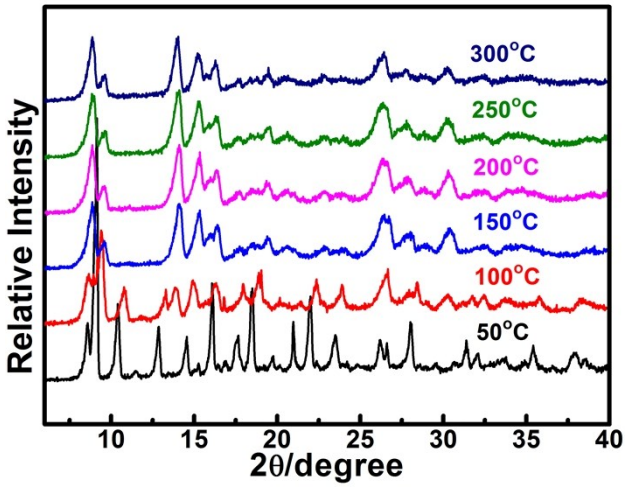

Fig. S6 Temperature-dependent PXRD pattern of compound **2**.

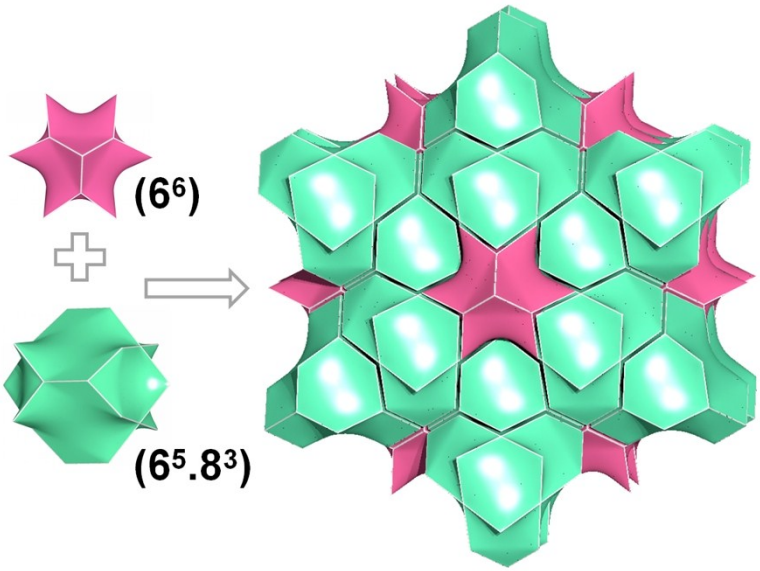

Fig. S7 Topological feature of compound **1** displayed by tiles and face symbols for pink and green tiles are (6^6) and ($6^5{\cdot}8^3$).

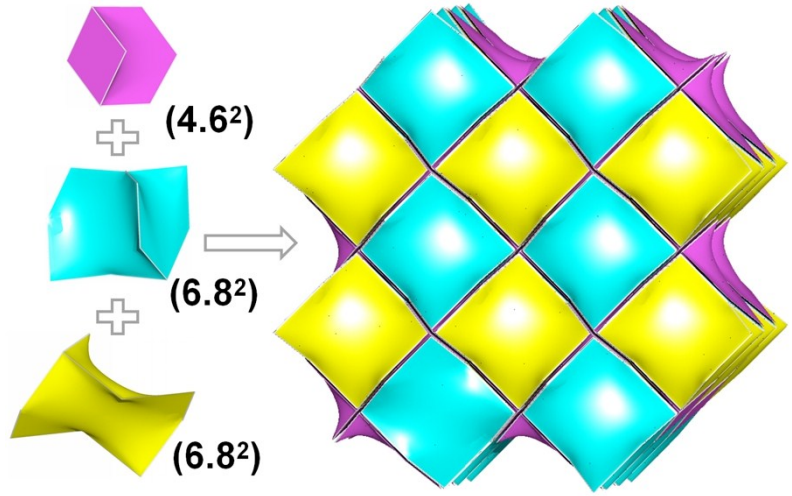

Fig. S8 Topological feature of compound **2** displayed by tiles and face symbols for pink, blue and yellow tiles are ($4{\cdot}6^2$), ($6{\cdot}8^2$) and ($6{\cdot}8^2$).

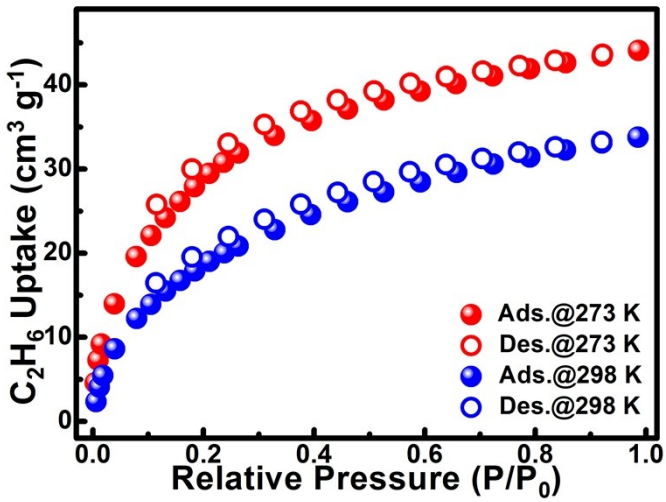

Fig. S9 C_2H_6 sorption isotherms for compound **1** at 273 and 298 K.

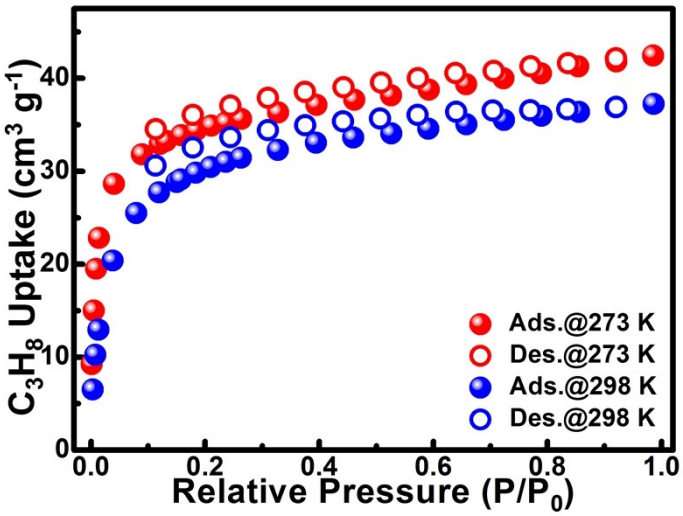

Fig. S10 C_3H_8 sorption isotherms for compound **1** at 273 and 298 K.

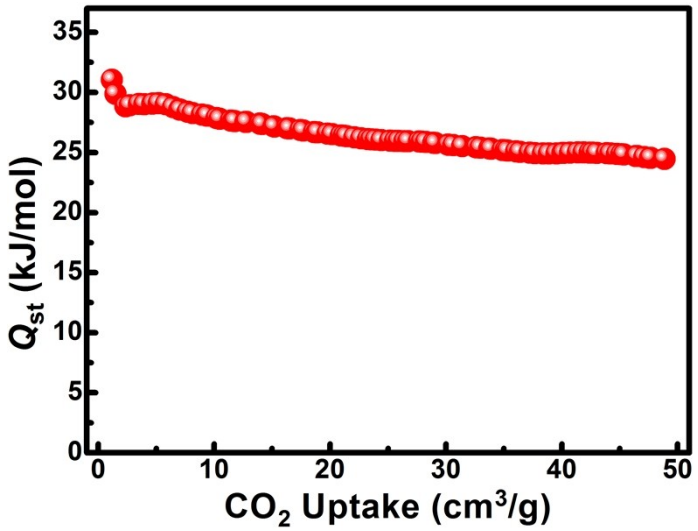

Fig. S11 Q_{st} of CO_2 for compound **1** calculated by MicroActive soft.

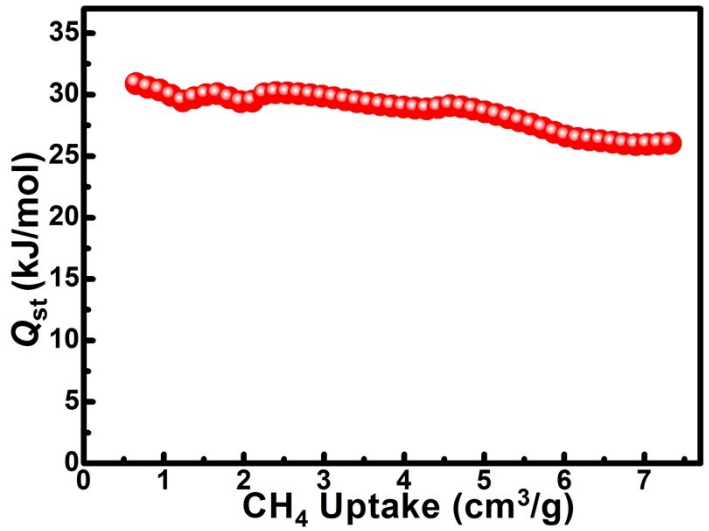

Fig. S12 Q_{st} of CH_4 for compound **1** calculated by MicroActive soft.

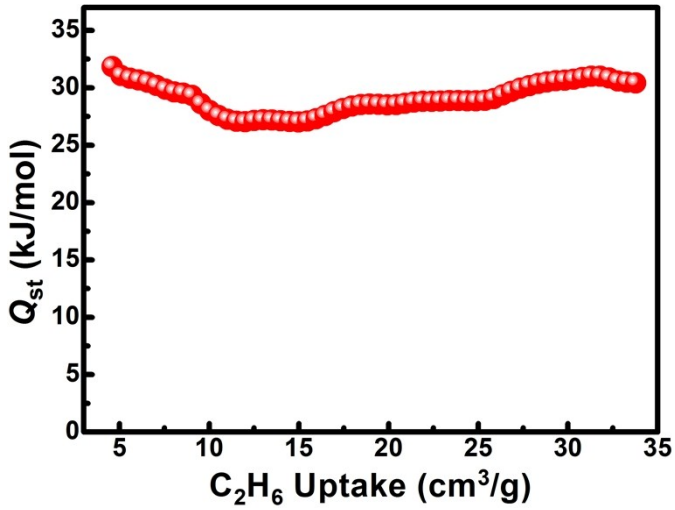

Fig. S13 Q_{st} of C_2H_6 for compound **1** calculated by MicroActive soft.

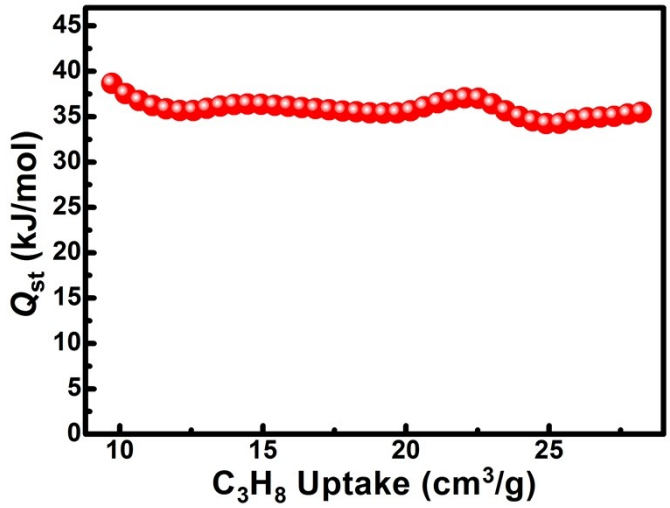

Fig. S14 Q_{st} of C_3H_8 for compound **1** calculated by MicroActive soft.

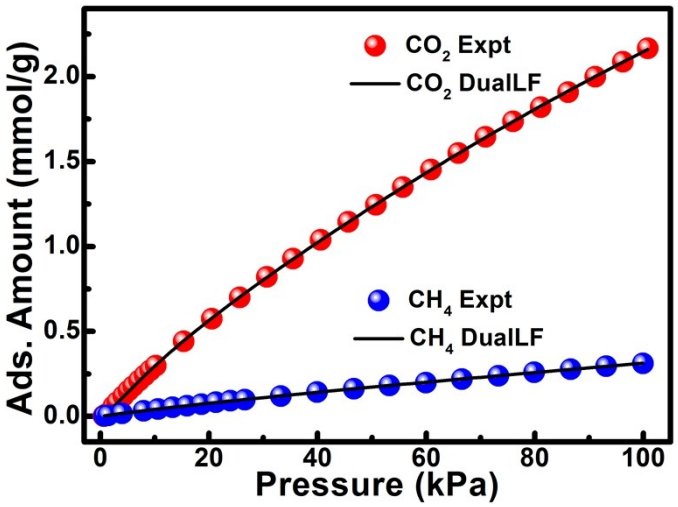

Fig. S15 CO_2 and CH_4 adsorption isotherms for compound **1** at 298 K along with the dual-site Langmuir Freundlich (DSLF) fits.

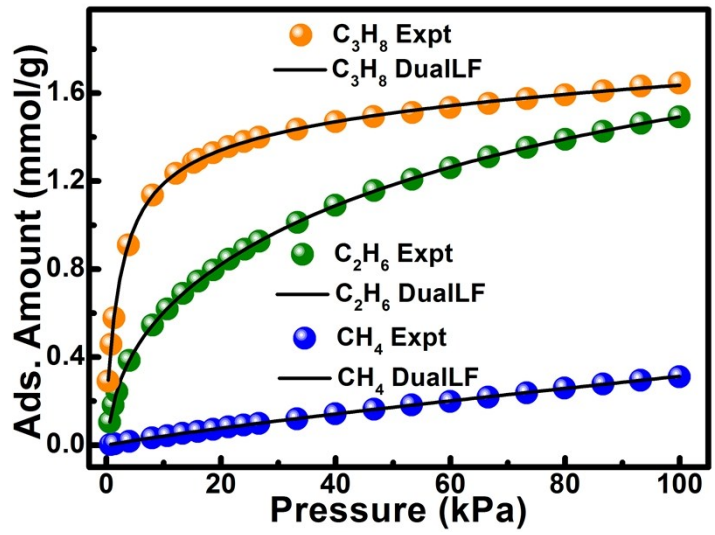

Fig. S16 C_2H_6, C_3H_8 and CH_4 adsorption isotherms for compound **1** at 298 K along with the dual-site Langmuir Freundlich (DSLF) fits.

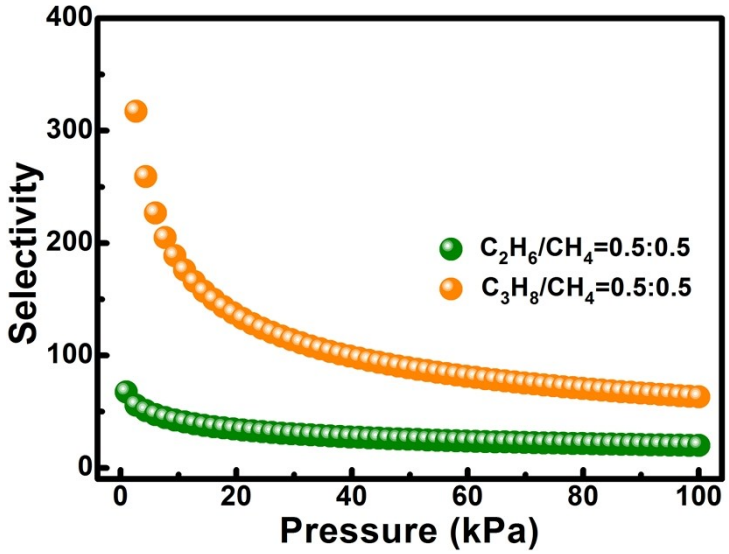

Fig. S17 C_2H_6, C_3H_8 and CH_4 gas mixture adsorption selectivity is predicted by IAST at 298 K and 100 kPa for compound **1**.

S3. Supporting Tables

Table S1. Crystal data and structure refinements for compound **1**and compound **2**.

Compound	**1**	**2**
Formula	$C_{25}H_{43}Cu_2ClN_8O_{10}$	$C_{30}H_{40}Cu_4N_{12}O_{16}$
F_w	778.20	1078.90
Temp (K)	293(2) K	293(2) K
Crystal system	Trigonal	Monoclinic
Space group	*P*-3m1	*P*2(1)/n
a (Å)	18.429(3)	12.009(2)
b (Å)	18.429(3)	11.479(2)
c (Å)	15.739(3)	16.743(3)
α (°)	90	90
β (°)	90	93.26(3)
γ (°)	120	90
V(Å^3)	4629.0(13)	2304.2(8)
Z	6	2
D_c (Mg m^{-3})	1.675	1.555
Absorption coefficient (mm^{-1})	1.534	1.896
F(000)	2424	1096
Reflections collected/unique (R_{int})	30705 / 3034 [R(int) = 0.0576]	14898/4171 [R(int) = 0.0413]
Goodness on fit	1.115	1.170
Final R indices [I > 2σ(I)]	R1 = 0.0383, wR2 = 0.1321	R1 = 0.0292, wR2 = 0.0909
R indices (all data)	R1 = 0.0490, wR2 = 0.1358	R1 = 0.0349, wR2 = 0.0921

$R_1=\sum||F_o|-|F_c||/\sum|F_o|$. $wR_2=[\sum[\ w\ (F_o^2-F_c^2)^2]\ /\ \sum[\ w\ (F_o^2)^2]]^{1/2}$

As the guest molecules were highly disordered and could not be modeled properly, the diffused electron densities resulting from them were removed by the SQUEEZE routine in PLATON and the results were appended in the following:

For compound **1**:

```
loop_
   _platon_squeeze_void_nr
   _platon_squeeze_void_average_x
   _platon_squeeze_void_average_y
   _platon_squeeze_void_average_z
   _platon_squeeze_void_volume
   _platon_squeeze_void_count_electrons
   _platon_squeeze_void_content
    1 -0.005    0.476 -0.014          3001          591 ' '
_platon_squeeze_void_probe_radius                    1.20
_platon_squeeze_details                              ?
```

For compound **2**:

```
loop_
   _platon_squeeze_void_nr
   _platon_squeeze_void_average_x
   _platon_squeeze_void_average_y
   _platon_squeeze_void_average_z
   _platon_squeeze_void_volume
   _platon_squeeze_void_count_electrons
   _platon_squeeze_void_content
     1 -0.007 -0.020    0.002          1339          282 ' '
_platon_squeeze_void_probe_radius                    1.20
_platon_squeeze_details                              ?
```

Table S2. Selected bond lengths [Å] and angles [°] for compound **1**.

Compound 1			
Cu(1)-O(2)#1	1.952(2)	Cu(1)-O(2)#2	1.952(2)
Cu(1)-O(1)#3	1.953(2)	Cu(1)-O(1)	1.953(2)
Cu(1)-O(3)	2.158(4)	Cu(1)-Cu(1)#1	2.6678(10)
Cu(2)-N(1)#4	1.969(3)	Cu(2)-N(1)	1.969(3)
Cu(2)-O(4')	2.16(2)	Cu(2)-O(4')#4	2.16(2)
Cu(2)-O(4)	2.294(14)	Cu(2)-O(4)#4	2.294(14)
Cu(2)-Cl(2)#5	2.301(3)	Cu(2)-Cl(2)	2.301(3)
Cu(2)-Cl(1)	2.393(2)	Cu(2)-Cl(1)#5	2.393(2)
Cl(1)-Cu(2)#6	2.393(2)	Cl(2)-Cu(2)#6	O(2)-Cu(1)#1
O(2)#1-Cu(1)-O(2)#2	88.86(16)	O(2)#1-Cu(1)-O(1)#3	89.58(12)
O(2)#2-Cu(1)-O(1)#3	167.31(10)	O(2)#1-Cu(1)-O(1)	167.31(10)
O(2)#2-Cu(1)-O(1)	89.58(12)	O(1)#3-Cu(1)-O(1)	89.19(16)
O(2)#1-Cu(1)-O(3)	97.28(12)	O(2)#2-Cu(1)-O(3)	97.28(12)
O(1)#3-Cu(1)-O(3)	95.41(12)	O(1)-Cu(1)-O(3)	95.41(12)
O(2)#1-Cu(1)-Cu(1)#1	82.91(7)	O(2)#2-Cu(1)-Cu(1)#1	82.91(7)
O(1)#3-Cu(1)-Cu(1)#1	84.40(7)	O(1)-Cu(1)-Cu(1)#1	84.40(7)
O(3)-Cu(1)-Cu(1)#1	179.72(15)	N(1)#4-Cu(2)-N(1)	178.87(18)
N(1)#4-Cu(2)-O(4')	86.6(5)	N(1)-Cu(2)-O(4')	92.3(5)
N(1)#4-Cu(2)-O(4')#4	92.3(5)	N(1)-Cu(2)-O(4')#4	86.6(5)
O(4')-Cu(2)-O(4')#4	40.1(9)	N(1)#4-Cu(2)-O(4)	90.5(7)
N(1)-Cu(2)-O(4)	88.4(7)	O(4')-Cu(2)-O(4)	25.8(8)
O(4')#4-Cu(2)-O(4)	14.4(5)	N(1)#4-Cu(2)-O(4)#4	88.4(7)
N(1)-Cu(2)-O(4)#4	90.5(7)	O(4')-Cu(2)-O(4)#4	14.4(5)
O(4')#4-Cu(2)-O(4)#4	25.8(8)	O(4)-Cu(2)-O(4)#4	11.4(10)
N(1)#4-Cu(2)-Cl(2)#5	89.55(12)	N(1)-Cu(2)-Cl(2)#5	91.26(13)
O(4')-Cu(2)-Cl(2)#5	115.9(5)	O(4')#4-Cu(2)-Cl(2)#5	155.6(5)
O(4)-Cu(2)-Cl(2)#5	141.4(5)	O(4)#4-Cu(2)-Cl(2)#5	130.2(5)
N(1)#4-Cu(2)-Cl(2)	91.26(13)	N(1)-Cu(2)-Cl(2)	89.55(12)
O(4')-Cu(2)-Cl(2)	155.6(5)	O(4')#4-Cu(2)-Cl(2)	115.9(5)
O(4)-Cu(2)-Cl(2)	130.2(5)	O(4)#4-Cu(2)-Cl(2)	141.4(5)
Cl(2)#5-Cu(2)-Cl(2)	88.4(4)	N(1)#4-Cu(2)-Cl(1)	91.94(11)
N(1)-Cu(2)-Cl(1)	88.43(10)	O(4')-Cu(2)-Cl(1)	129.3(4)
O(4')#4-Cu(2)-Cl(1)	89.4(4)	O(4)-Cu(2)-Cl(1)	103.7(5)
O(4)#4-Cu(2)-Cl(1)	115.0(5)	Cl(2)#5-Cu(2)-Cl(1)	114.8(3)
Cl(2)-Cu(2)-Cl(1)	26.42(16)	N(1)#4-Cu(2)-Cl(1)#5	88.43(10)
N(1)-Cu(2)-Cl(1)#5	91.94(11)	O(4')-Cu(2)-Cl(1)#5	89.4(4)
O(4')#4-Cu(2)-Cl(1)#5	129.3(4)	O(4)-Cu(2)-Cl(1)#5	115.0(5)
O(4)#4-Cu(2)-Cl(1)#5	103.7(5)	Cl(2)#5-Cu(2)-Cl(1)#5	26.42(16)
Cl(2)-Cu(2)-Cl(1)#5	114.8(3)	Cl(1)-Cu(2)-Cl(1)#5	141.2(2)
Cu(2)-Cl(1)-Cu(2)#6	100.45(12)	Cu(2)#6-Cl(2)-Cu(2)	106.12(17)
C(6)-O(1)-Cu(1)	122.4(2)	C(6)-O(2)-Cu(1)#1	124.4(2)

O(4)#4-O(4)-Cu(2)	84.3(5)	O(4')#4-O(4')-Cu(2)	69.9(4)
N(1)#7-N(1)-Cu(2)	126.89(8)	N(2)-N(1)-Cu(2)	123.3(2)
N(1)#7-N(1)-N(2)	109.79(18)	N(2)-C(1)-N(2)#7	111.4(4)

Symmetry transformations used to generate equivalent atoms:

#1 -x+1,-y,-z+1 #2 x-y,-y,-z+1 #3 -x+y+1,y,z #4 x-y,-y,-z #5 y,-x+y,-z #6 x-y,x,-z #7 x,x-y,z

Table S3. Selected bond lengths [Å] and angles [°] for compound **2**.

Compound 2			
Cu(1)-O(3)#1	1.937(2)	Cu(1)-O(5)	1.967(2)
Cu(1)-O(5)#2	2.033(2)	Cu(1)-N(3)#3	2.041(3)
Cu(1)-O(1)	2.114(2)	Cu(1)-Cu(1)#2	3.0348(10)
Cu(2)-O(4)#4	1.950(2)	Cu(2)-O(5)	1.952(2)
Cu(2)-O(6)	1.970(3)	Cu(2)-N(2)#3	2.004(3)
Cu(2)-O(2)#2	2.177(3)	O(2)-Cu(2)#2	2.177(3)
O(3)-Cu(1)#5	1.937(2)	O(4)-Cu(2)#6	1.950(2)
O(5)-Cu(1)#2	2.033(2)	N(2)-Cu(2)#7	2.004(3)
N(3)-Cu(1)#7	2.041(3)	O(3)#1-Cu(1)-O(5)	173.84(10)
O(3)#1-Cu(1)-O(5)#2	94.42(9)	O(5)-Cu(1)-O(5)#2	81.30(9)
O(3)#1-Cu(1)-N(3)#3	92.36(10)	O(5)-Cu(1)-N(3)#3	88.37(9)
O(5)#2-Cu(1)-N(3)#3	141.91(10)	O(3)#1-Cu(1)-O(1)	91.16(11)
O(5)-Cu(1)-O(1)	94.45(10)	O(5)#2-Cu(1)-O(1)	109.73(9)
N(3)#3-Cu(1)-O(1)	107.54(11)	O(3)#1-Cu(1)-Cu(1)#2	134.10(7)
O(5)-Cu(1)-Cu(1)#2	41.46(6)	O(5)#2-Cu(1)-Cu(1)#2	39.84(6)
N(3)#3-Cu(1)-Cu(1)#2	120.59(8)	O(1)-Cu(1)-Cu(1)#2	106.05(7)
O(4)#4-Cu(2)-O(5)	93.98(10)	O(4)#4-Cu(2)-O(6)	84.81(11)
O(5)-Cu(2)-O(6)	170.16(12)	O(4)#4-Cu(2)-N(2)#3	166.49(12)
O(5)-Cu(2)-N(2)#3	87.68(11)	O(6)-Cu(2)-N(2)#3	91.27(12)
O(4)#4-Cu(2)-O(2)#2	102.28(11)	O(5)-Cu(2)-O(2)#2	93.32(10)
O(6)-Cu(2)-O(2)#2	96.48(13)	N(2)#3-Cu(2)-O(2)#2	91.00(11)
C(8)-O(1)-Cu(1)	120.3(2)	C(8)-O(2)-Cu(2)#2	123.3(2)
C(9)-O(3)-Cu(1)#5	122.7(2)	C(9)-O(4)-Cu(2)#6	135.5(2)
Cu(2)-O(5)-Cu(1)	113.81(10)	Cu(2)-O(5)-Cu(1)#2	106.15(10)
Cu(1)-O(5)-Cu(1)#2	98.70(9)	Cu(2)-O(5)-H(5A)	Cu(1)-O(5)-H(5A)
Cu(1)#2-O(5)-H(5A)	118(2)	N(3)-N(2)-Cu(2)#7	120.0(2)
N(1)-N(2)-Cu(2)#7	128.6(2)	N(2)-N(3)-Cu(1)#7	117.71(19)
N(4)-N(3)-Cu(1)#7	132.7(2)	C(10)-O(6)-Cu(2)	125.5(5)
C(10')-O(6)-Cu(2)	117.8(13)	N(3)-N(2)-N(1)	110.2(2)

Symmetry transformations used to generate equivalent atoms:

#1 -x+1/2,y-1/2,-z+1/2 #2 -x+1,-y+2,-z+1 #3 x-1/2,-y+5/2,z+1/2 #4 x+1/2,-y+5/2,z+1/2

#5 -x+1/2,y+1/2,-z+1/2 #6 x-1/2,-y+5/2,z-1/2 #7 x+1/2,-y+5/2,z-1/2

Table S4. The refined parameters for the Dual-site Langmuir-Freundlich equations fit for the pure isotherms of CO_2, CH_4, C_2H_6 and C_3H_8 for compound **1** at 298 K.

	q_{m1}	b_1	n_1	q_{m2}	b_2	n_2	R^2
CO_2	0.34564	0.02986	1.38831	6.4509	0.00145	1.21709	0.99996
CH_4	0.01724	0.02279	1.5	4.52556	8.14096E-4	0.96731	0.99982
C_2H_6	0.11586	0.47064	1.55686	2.70934	0.04821	0.66536	0.99998
C_3H_8	0.34162	0.29103	1.5	1.63897	0.36175	0.5	0.99925

Table S5. Comparison of compound **1** with other MOFs which exhibits high selectivity for CO_2 over CH_4 at 298 K under 1 bar.

Compound	Selectivity	Reference
ZJNU-55a	13.1	1
Mg-MOF-74	11.5	2
JLU-Liu46	9.8	3
Compound 1	**9.6**	**This work**
JLU-Liu22	9.4	4
Cu-PEIP	8.9	5
JLU-Liu6	7.4	6
JLU-Liu20	5.9	7
ZJNU-84	5.85	8
JLU-Liu2	4	9
MOF-5	2.3	10
MIL-53(Al)	2.3	11
$Cu_3(BTC)_2$	2.3	11
UMCM-1	1.8	11
MOF-177	0.9	11

Reference:

1. J. Jiao, H. Liu, F. Chen, D. Bai, S. Xiong and Y. He, *Inorg. Chem. Front.*, 2016, **3**, 1411-1418.
2. S. R. Caskey, A. G. Wong-Foy, and A. J. Matzger, *J. Am. Chem. Soc.*, 2008, **130**, 10870-

10871.
3. B. Liu, S. Yao, X. Liu, Xu. Li, R. Krishna, G. Li, Q. Huo and Y. Liu, *ACS Appl. Mater. Interfaces*, 2017, **9**, 32820-32828.
4. D. Wang, B. Liu, S. Yao, T. Wang, G. Li, Q. Huo and Y. Liu, *Chem. Commun.*, 2015, **51**, 15287-15289.
5. A. Kourtellaris, E. E. Moushi, I. Spanopoulos, C. Tampaxis, G. Charalambopoulou,T. A. Steriotis, G. S. Papaefstathiou, P. N. Trikalitis and A. J. Tasiopoulos, *Inorg. Chem. Front.*, 2016, **3**, 1527-1535.
6. D. Wang, T. Zhao, Y. Cao, S. Yao, G. Li, Q. Huo and Y. Liu, *Chem. Commun.,* 2014, **50**, 8648-8650.
7. B. Liu, S. Yao, C. Shi, G. Li, Q. Huo and Y. Liu, *Chem. Commun.,* 2016, **52**, 3223-3226.
8. D. Bai, X. Gao, M. He, Y. Wang and Y. He, *Inorg. Chem. Front.*, 2018, **5**, 1423-1431.
9. D. Wang, T. Zhao, G. Li, Q. Huo and Y. Liu, *Dalton Trans.*, 2014, **43**, 2365-2368.
10. Z. Zhang, S. Xiang, K. Hong, M. C. Das, H. D. Arman, M. Garcia, J. U. Mondal, K. M. Thomas and B. Chen, *Inorg. Chem.,* 2012, **51**, 4947−4953.
11. Z. H. Xiang, X. Peng, X. Cheng, X. J. Li and D. P. Cao, *J. Phys. Chem. C*, 2011, **115**, 19864-19871.